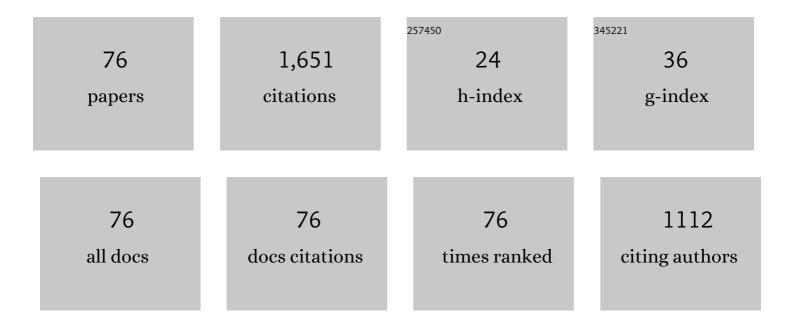
List of Publications by Year in descending order

Source: https://exaly.com/author-pdf/2444316/publications.pdf Version: 2024-02-01



#	Article	IF	CITATIONS
1	Was Magnetic Storm the Only Driver of the Longâ€Duration Enhancements of Daytime Total Electron Content in the Asianâ€Australian Sector Between 7 and 12 September 2017?. Journal of Geophysical Research: Space Physics, 2018, 123, 3217-3232.	2.4	87
2	Statistics of GPS ionospheric scintillation and irregularities over polar regions at solar minimum. GPS Solutions, 2010, 14, 331-341.	4.3	73
3	Precursor signatures and evolution of postâ€sunset equatorial spreadâ€F observed over Sanya. Journal of Geophysical Research, 2012, 117, .	3.3	64
4	Effects of disturbed electric fields in the low″atitude and equatorial ionosphere during the 2015 St. Patrick's Day storm. Journal of Geophysical Research: Space Physics, 2016, 121, 9111-9126.	2.4	60
5	Tidal wind mapping from observations of a meteor radar chain in December 2011. Journal of Geophysical Research: Space Physics, 2013, 118, 2321-2332.	2.4	58
6	On the occurrence of postmidnight equatorial <i>F</i> region irregularities during the June solstice. Journal of Geophysical Research, 2011, 116, n/a-n/a.	3.3	56
7	GPS TEC response to the 22 July 2009 total solar eclipse in East Asia. Journal of Geophysical Research, 2010, 115, .	3.3	52
8	A case study of postmidnight enhancement in Fâ€layer electron density over Sanya of China. Journal of Geophysical Research: Space Physics, 2013, 118, 4640-4648.	2.4	51
9	The global climatology of the intensity of the ionospheric sporadic <i>E</i> layer. Atmospheric Chemistry and Physics, 2019, 19, 4139-4151.	4.9	51
10	Longâ€lasting negative ionospheric storm effects in low and middle latitudes during the recovery phase of the 17 March 2013 geomagnetic storm. Journal of Geophysical Research: Space Physics, 2016, 121, 9234-9249.	2.4	49
11	Longitudinal development of low″atitude ionospheric irregularities during the geomagnetic storms of July 2004. Journal of Geophysical Research, 2010, 115, .	3.3	44
12	Statistical characteristics of low-latitude ionospheric scintillation over China. Advances in Space Research, 2015, 55, 1356-1365.	2.6	41
13	The first time observations of low-latitude ionospheric irregularities by VHF radar in Hainan. Science China Technological Sciences, 2012, 55, 1189-1197.	4.0	36
14	Development of the Beidou Ionospheric Observation Network in China for space weather monitoring. Space Weather, 2017, 15, 974-984.	3.7	31
15	Highâ€speed stream impacts on the equatorial ionization anomaly region during the deep solar minimum year 2008. Journal of Geophysical Research, 2012, 117, .	3.3	30
16	Validation of COSMIC ionospheric peak parameters by the measurements of an ionosonde chain in China. Annales Geophysicae, 2014, 32, 1311-1319.	1.6	29
17	Interferometry observations of low-latitude E-region irregularity patches using the Sanya VHF radar. Science China Technological Sciences, 2014, 57, 1552-1561.	4.0	29
18	A statistic study of ionospheric solar flare activity indicator. Space Weather, 2014, 12, 29-40.	3.7	28

#	Article	IF	CITATIONS
19	Investigation of ionospheric TEC over China based on GNSS data. Advances in Space Research, 2016, 58, 867-877.	2.6	26
20	Low Latitude Ionospheric TEC Oscillations Associated With Periodic Changes in IMF Bz Polarity. Geophysical Research Letters, 2019, 46, 9379-9387.	4.0	26
21	IONISE: An Ionospheric Observational Network for Irregularity and Scintillation in East and Southeast Asia. Journal of Geophysical Research: Space Physics, 2020, 125, e2020JA028055.	2.4	26
22	Investigation of low-latitude <i>E</i> and valley region irregularities: Their relationship to equatorial plasma bubble bifurcation. Journal of Geophysical Research, 2011, 116, n/a-n/a.	3.3	25
23	A comparison of mesospheric winds measured by FPI and meteor radar located at 40N. Science China Technological Sciences, 2012, 55, 1245-1250.	4.0	25
24	Comparison between ionospheric peak parameters retrieved from COSMIC measurement and ionosonde observation over Sanya. Advances in Space Research, 2014, 54, 929-938.	2.6	25
25	Seasonal variations of MLT tides revealed by a meteor radar chain based on Hough mode decomposition. Journal of Geophysical Research: Space Physics, 2015, 120, 7030-7048.	2.4	25
26	On the linkage of daytime 150 km echoes and abnormal intermediate layer traces over Sanya. Journal of Geophysical Research: Space Physics, 2013, 118, 7262-7267.	2.4	24
27	Mapping the conjugate and corotating stormâ€enhanced density during 17 March 2013 storm through data assimilation. Journal of Geophysical Research: Space Physics, 2016, 121, 12,202.	2.4	24
28	Evidence for lightningâ€associated enhancement of the ionospheric sporadic <i>E</i> layer dependent on lightning stroke energy. Journal of Geophysical Research: Space Physics, 2015, 120, 9202-9212.	2.4	23
29	Regional differences of the ionospheric response to the July 2012 geomagnetic storm. Journal of Geophysical Research: Space Physics, 2017, 122, 4654-4668.	2.4	23
30	Comparison of the ionospheric F2 peak height between ionosonde measurements and IRI2016 predictions over China. Advances in Space Research, 2017, 60, 1524-1531.	2.6	22
31	Observations and modeling of the ionospheric behaviors over the east Asia zone during the 22 July 2009 solar eclipse. Journal of Geophysical Research, 2010, 115, .	3.3	21
32	Mesospheric temperatures estimated from the meteor radar observations at Mohe, China. Journal of Geophysical Research: Space Physics, 2017, 122, 2249-2259.	2.4	21
33	Contrasting behavior of the F 2 peak and the topside ionosphere in response to the 2 October 2013 geomagnetic storm. Journal of Geophysical Research: Space Physics, 2016, 121, 10,549-10,563.	2.4	20
34	Two Day Wave Traveling Westward With Wave Number 1 During the Sudden Stratospheric Warming in January 2017. Journal of Geophysical Research: Space Physics, 2018, 123, 3005-3013.	2.4	19
35	A comparison of lower thermospheric winds derived from range spread and specular meteor trail echoes. Journal of Geophysical Research, 2012, 117, .	3.3	18
36	Largeâ€6cale Structure of Subauroral Polarization Streams During the Main Phase of a Severe Geomagnetic Storm. Journal of Geophysical Research: Space Physics, 2018, 123, 2964-2973.	2.4	18

#	Article	lF	CITATIONS
37	Ionospheric response following the <i>M</i> _{<i>w</i>} 7.8 Gorkha earthquake on 25 April 2015. Journal of Geophysical Research: Space Physics, 2017, 122, 6495-6507.	2.4	17
38	Variations of the meteor echo heights at Beijing and Mohe, China. Journal of Geophysical Research: Space Physics, 2017, 122, 1117-1127.	2.4	16
39	Strong Sporadic <i>E</i> Occurrence Detected by Groundâ€Based GNSS. Journal of Geophysical Research: Space Physics, 2018, 123, 3050-3062.	2.4	15
40	Ionospheric Trend Over Wuhan During 1947–2017: Comparison Between Simulation and Observation. Journal of Geophysical Research: Space Physics, 2018, 123, 1396-1409.	2.4	15
41	Persistence of the Longâ€Duration Daytime TEC Enhancements at Different Longitudinal Sectors During the August 2018 Geomagnetic Storm. Journal of Geophysical Research: Space Physics, 2020, 125, e2020JA028238.	2.4	15
42	Morphological Characteristics of Thousandâ€Kilometerâ€Scale E _s Structures Over China. Journal of Geophysical Research: Space Physics, 2021, 126, e2020JA028712.	2.4	15
43	Daytime F-region irregularity triggered by rocket-induced ionospheric hole over low latitude. Progress in Earth and Planetary Science, 2018, 5, .	3.0	14
44	New Approach to Estimate Tidal Climatology From Ground―and Spaceâ€Based Observations. Journal of Geophysical Research: Space Physics, 2018, 123, 5087-5101.	2.4	14
45	Unseasonal super ionospheric plasma bubble and scintillations seeded by the 2022 Tonga Volcano Eruption related perturbations. Journal of Space Weather and Space Climate, 2022, 12, 25.	3.3	14
46	Observation of Shortâ€Period Ionospheric Disturbances Using a Portable Digital Ionosonde at Sanya. Radio Science, 2018, 53, 1521-1532.	1.6	13
47	Unexpected High Occurrence of Daytime Fâ€Region Backscatter Plume Structures Over Low Latitude Sanya and Their Possible Origin. Geophysical Research Letters, 2020, 47, e2020GL090517.	4.0	13
48	Deep-learning for ionogram automatic scaling. Advances in Space Research, 2020, 66, 942-950.	2.6	13
49	Midlatitudinal Special Airglow Structures Generated by the Interaction Between Propagating Mediumâ€Scale Traveling Ionospheric Disturbance and Nighttime Plasma Density Enhancement at Magnetically Quiet Time. Geophysical Research Letters, 2019, 46, 1158-1167.	4.0	12
50	Statistical Characteristics and Correlation of Low‣atitude F Region Bottomâ€Type Irregularity Layers and Plasma Plumes Over Sanya. Journal of Geophysical Research: Space Physics, 2020, 125, e2020JA027855.	2.4	12
51	The possibility of using all-sky meteor radar to observe ionospheric E-region field-aligned irregularities. Science China Technological Sciences, 2019, 62, 1431-1437.	4.0	11
52	The intensification of metallic layered phenomena above thunderstorms through the modulation of atmospheric tides. Scientific Reports, 2019, 9, 17907.	3.3	10
53	Estimation of Ionospheric Total Electron Content From a Multi-GNSS Station in China. IEEE Transactions on Geoscience and Remote Sensing, 2020, 58, 852-860.	6.3	10
54	A case study of ionospheric storm effects in the Chinese sector during the October 2013 geomagnetic storm. Advances in Space Research, 2015, 56, 2030-2039.	2.6	9

#	Article	IF	CITATIONS
55	Structures of Multiple Largeâ€5cale Traveling Ionospheric Disturbances Observed by Dense Global Navigation Satellite System Networks in China. Journal of Geophysical Research: Space Physics, 2020, 125, e2019JA027032.	2.4	9
56	The Prediction of Dayâ€ŧoâ€Ðay Occurrence of Low Latitude Ionospheric Strong Scintillation Using Gradient Boosting Algorithm. Space Weather, 2021, 19, e2021SW002884.	3.7	9
57	Observing System Impact on Ionospheric Specification Over China Using EnKF Assimilation. Space Weather, 2020, 18, e2020SW002527.	3.7	8
58	The Evolution of Complex E s Observed by Multi Instruments Over Low‣atitude China. Journal of Geophysical Research: Space Physics, 2020, 125, e2019JA027656.	2.4	8
59	The Ionosphere at Middle and Low Latitudes Under Geomagnetic Quiet Time of December 2019. Journal of Geophysical Research: Space Physics, 2021, 126, e2020JA028964.	2.4	8
60	Occurrence and Variations of Middle and Low Latitude Sporadic E Layer Investigated With Longitudinal and Latitudinal Chains of Ionosondes. Space Weather, 2021, 19, e2021SW002942.	3.7	8
61	Design of Meteor and Ionospheric Irregularity Observation System and First Results. Journal of Geophysical Research: Space Physics, 2022, 127, .	2.4	8
62	Observational evidence of highâ€altitude meteor trail from radar interferometer. Geophysical Research Letters, 2014, 41, 6583-6589.	4.0	7
63	Shear in the zonal drifts of 3 m irregularities inside spread <i>F</i> plumes observed over Sanya. Journal of Geophysical Research: Space Physics, 2015, 120, 8146-8154.	2.4	7
64	Response of the equatorial and low-latitude ionosphere over the West Pacific Ocean Sector to an X1.2 solar flare on 15 May 2013. Advances in Space Research, 2017, 60, 1029-1038.	2.6	7
65	Interaction Between a Southwestward Propagating MSTID and a Poleward Moving WSAâ€Like Plasma Patch on a Magnetically Quiet Night at Midlatitude China Region. Journal of Geophysical Research: Space Physics, 2020, 125, e2020JA028085.	2.4	7
66	Climatology of equatorial and low-latitude F region kilometer-scale irregularities over the meridian circle around 120°E/60°W. GPS Solutions, 2021, 25, 1.	4.3	7
67	Latitudinal Variations of Daytime Periodic Ionospheric Disturbances From Beidou GEO TEC Observations Over China. Journal of Geophysical Research: Space Physics, 2021, 126, e2020JA028809.	2.4	7
68	Statistical Study on the Occurrences of Postsunset Ionospheric E , Valley, and F Region Irregularities and Their Correlations Over Low‣atitude Sanya. Journal of Geophysical Research: Space Physics, 2018, 123, 9873-9880.	2.4	5
69	MIOS optical subsystem for determining physical and chemical properties of meteors producing plasma irregularities. Advances in Space Research, 2021, 68, 1556-1567.	2.6	5
70	Occurrences of regional strong E s irregularities and corresponding scintillations characterized using a highâ€ŧemporalâ€resolution GNSS network. Journal of Geophysical Research: Space Physics, 0, , .	2.4	5
71	Daytime Ionospheric Largeâ€Scale Plasma Density Depletion Structures Detected at Low Latitudes Under Relatively Quiet Geomagnetic Conditions. Journal of Geophysical Research: Space Physics, 2022, 127, .	2.4	5
72	Global tidal mapping from observations of a radar campaign. Advances in Space Research, 2017, 60, 130-143.	2.6	4

#	Article	IF	CITATIONS
73	Dayâ€Toâ€Day Variability of the MLT DE3 Using Joint Analysis on Observations From TIDIâ€TIMED and a Meteor Radar Meridian Chain. Journal of Geophysical Research D: Atmospheres, 2022, 127, .	3.3	3
74	Seasonal variations of night mesopause temperature in Beijing observed by SATI4. Science China Technological Sciences, 2012, 55, 1295-1301.	4.0	2
75	GPS network observation of traveling ionospheric disturbances following the Chelyabinsk meteorite blast. Annales Geophysicae, 2016, 34, 1045-1051.	1.6	2
76	Onset location of scintillation-producing spread-F plume over Sanya. Science China Earth Sciences, 2016, 59, 1692-1699.	5.2	2